ELSEVIER

Catalysis Today 70 (2001) 15–31

CATALYSIS TODAY

www.elsevier.com/locate/cattod

Reactivity of SO_2 and NH_3 on copper well-defined surfaces: an IRAS investigation

C.M. Pradier

Laboratoire de Physico-Chimie des Surfaces, ESA 7045, Ecole Nationale Supérieure de Chimie de Paris, 11 rue P.et M. Curie, 75005 Paris, France

Abstract

FT-IR spectroscopy has been used in the reflection mode on metal surfaces to in situ investigate several systems involved in the current catalytic processes as well as in environment-related problems. The reactivity of SO_2, $SO_2 + O_2$, $SO_2 + H_2O$, $SO_2 + i\text{-}C_4H_8$ and also NH_3 with well controlled copper surfaces has been monitored by IRAS at room temperature in the presence of reactants ($P = 10^{-5}$–10^{-4} Torr). Various molecular surface complexes have been identified; their geometry and binding mode have been deduced from the position and the number of vibration bands. Both the reactivities of SO_2 and NH_3 appear to be highly sensitive to the structure and to the level of oxidation of the surface.

SO_2 mostly dissociates on metallic copper; it does react with adsorbed oxygen or lattice oxygen of an oxide layer and leads to sulphites and sulphates coordinated to the surface via oxygen. As an example, on Cu(1 1 0), bidentate sulphates are predominant when oxygen is adsorbed and mobile on the surface; conversely, monodentate sulphites are formed by interaction of SO_2 molecules with lattice surface oxygen. A similar evolution was observed on Cu(1 0 0). NH_3 is adsorbed on Cu(1 1 0) and, in the presence of oxygen in the gas phase, Cu–NH_2, Cu–NH species are detected on the surface as intermediates of the selective oxidation of NH_3 into N_2. In the presence of water, SO_2 leads to complex species; hydrogen-sulphates are formed by an electrophilic attack of OH groups by the S atom of SO_2. Finally, the interaction of SO_2 and $i\text{-}C_4H_8$ with Cu(1 1 0) has revealed that these two species co-adsorb and react in the adsorbed layer. These results have been used to explain the mechanism of poisoning of the reduction of NO on copper in the presence of isobutene and oxygen. The data, here presented, show how performing the IRAS technique is for a real-time in situ monitoring of the reactivity of planar surfaces.

Keywords: FT-IRAS; Cu(1 1 0); Cu(1 0 0); SO_2; NH_3

1. Introduction

This contribution aims at presenting an original investigation of the reactivity of SO_2 and NH_3 with metallic or oxygen-modified well-defined copper surfaces. Fourier transform-infrared reflection absorption spectroscopy (FT-IRAS) has been applied in the 10^{-8}–10^{-3} Torr pressure range in order to obtain in situ measurements. Interpretations are based on structural considerations.

2. Infrared reflection at metal surfaces

IRAS has been widely used to determine the chemical nature and the structure of adsorbed molecular compounds on metal surfaces. Used in a single reflection mode, infrared is sensitive to submonolayer amounts of species. Moreover, conversely to most of

E-mail address: pradier@ext.jussieu.fr (C.M. Pradier).

0920-5861/01/$ – see front matter
PII: S0920-5861(01)00404-7

the surface characterisation techniques, this method can be performed in the presence of low or intermediate pressures of gases ($P = 10^{-9}$ Torr to the atmospheric pressure). These advantages make IRAS an in situ technique for the characterisation of reaction intermediates. It is a way to bridge surface studies, performed under UHV conditions and reactivity studies under catalytic relevant pressures.

2.1. Reflection at metal surfaces: theoretical considerations

The IRAS theory, first presented by Greenler [1], has been developed and exploited by several other authors. When an incident light is reflected at a metal surface, the resulting electric field is a linear combination of the incident and reflected fields. The phase shift, induced by reflection, is a function of the angle of incidence; it is almost equal to 180° for the component normal to the plane of incidence (destructive interference); it varies for the component parallel to the plane of incidence so that the light intensity, at the surface, is maximum at an angle of incidence just below 90°. Theoretical considerations remarkably developed by Greenler, and applied in the pioneer work of Bradshaw and Hoffmann [2,3], yield the two following important conclusions that have to be kept in mind:

- Only the component of the incident light with a polarisation parallel to the plane of incidence will yield a non-vanishing electric field at the surface and only vibrations with a dipole moment perpendicular to the surface will be excited (dipole selection rule).
- The light should hit the surface at grazing incidence.

For an adsorbate-covered surface, a three-phase model, taking the optical properties of the adsorbate into account, has been developed, which yields similar considerations concerning the incidence angle and light polarisation. Moreover, it has been shown that, except for highly reflecting noble metals like Ag, Au and Cu, single reflection is the most efficient configuration on most transition metals due to the energy loss accompanying multiple reflections. One consequence of these features is that, for a given molecule adsorbed on a metal surface, the signal intensity is dependent on its orientation towards the surface. This can be considered as an advantage of the technique since, in addition to a chemical characterisation, geometrical information can be drawn. Further insight into the intermolecular interactions within the adsorbed layer can be gained by observing the positions and the shifts of the vibration bands as a function of the coverage.

To conclude this short theoretical overview of the IRAS technique, let us keep in mind that the vibrational spectrum of adsorbed molecules brings various types of information related to:

- the nature of the molecular groups present in the adsorbed layer;
- the orientation and symmetry of the molecules by considering the number and position of the vibration bands;
- the strength of the metal-adsorbate bond by, in the most favourable cases, detecting a characteristic vibration band or observing shifts in the internal modes of the molecule;
- the structure and order within the adsorbed layer by considering the band width;
- the reactivity of molecules on a metal surface since the kinetics of formation and disappearance of molecular compounds can be monitored in the presence of a reactive gas mixture.

The technique has been successfully used to characterise the adsorption of CO on metal single crystal surfaces and determine the adsorption mode as well as site geometry [4]. Attempts have been made to correlate IRAS measurements at low and high pressures, on single crystals and divided surfaces [5]. More complex molecules can of course be similarly investigated; the assignments of the observed signal are more difficult unless it is possible to refer to data established for the analogous coordination complexes.

The two following examples, adsorption and reactivity of SO_2 and NH_3 with well-defined copper surfaces, investigated by FT-IRAS at pressure between 10^{-8} and 10^{-3} Torr, will illustrate some of the above mentioned points.

2.2. Experimental device

Several arrangements for IRAS measurements have been presented in the literature [3,6]. Most of them are part of a UHV system allowing surface characterisation by infrared or by more conventional surface characterisation techniques under vacuum (low energy

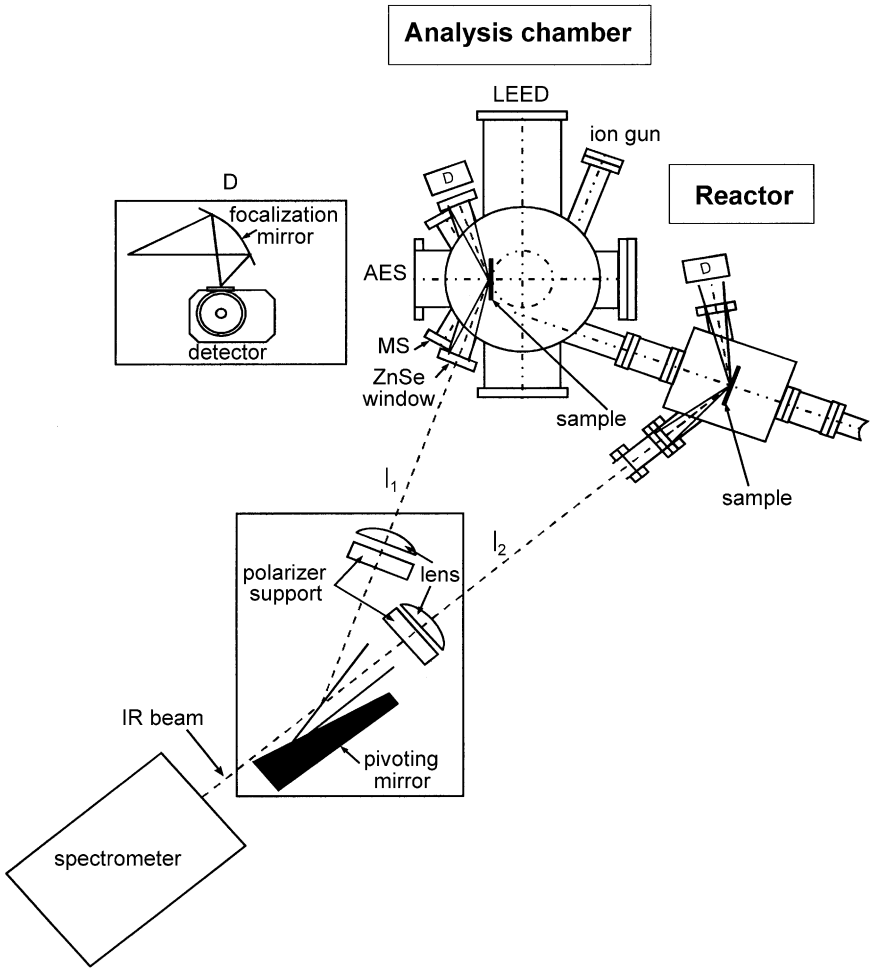

Fig. 1. Experimental device for FT-IRAS measurements at low and intermediate pressures.

electron diffraction (LEED) and Auger electron spectroscopy (AES)).

The system used for the experiments reported below is shown in Fig. 1. It is constituted of two chambers for IRAS analyses: one, in which only low-pressure ($P \leq 10^{-6}$ Torr) IR analyses are performed, is equipped with LEED, AES, and mass spectrometry for surface and gas control, respectively; a second one, of a smaller size for having an optical path as short as possible, equipped with a rapid load-in window for an easy change of the sample, in which the gas pressure can be raised up to the atmosphere. This second chamber is connected both to a glass circuit, constituting a batch catalytic reactor, and to the UHV chamber for the transfer of the sample and the control of the surface before and after each gas treatment. The crystal was fixed by tungsten wires that enable to heat it to 1200 K in a few seconds. In the UHV chamber, the crystal surface was cleaned by successive argon bombardment ($E = 200$ V at $P_{Ar} = 10^{-4}$ Torr), treatment under hydrogen at elevated temperature, and annealing under vacuum. All FT-IRAS measurements were performed with a NICOLET, Magna 550 spectrometer, at 4 cm^{-1} resolution, and using a nitrogen-cooled MCT detector. The beam, external to the spectrometer, was focused onto the sample surface by lenses. All the optical paths out of the chamber were purged with dry air. Six hundred scans were taken for each surface spectrum

and subtraction of the substrate spectrum, before gas admission (reference spectrum) was performed.

3. Two examples of applications

3.1. Interaction of SO_2 with well-defined copper surfaces

3.1.1. Interaction of SO_2 with copper, a brief literature review

Sulphur dioxide plays a determining role in various concerning domains, catalyst poisoning, environmental damage as well as atmospheric corrosion. SO_2 is a complex molecule since it can act as a Lewis base with a cation centre; it can also undergo a reduction through a nucleophilic attack of the S atom by an electron-rich atom (oxygen). The interaction of SO_2 with various metal surfaces has been characterised at a molecular level by advanced surface probes, HREELS, HR-XPS, LEED. It has been in particular established that, on Cu(1 0 0) and Cu(1 1 1), SO_2 can decompose and then react with O(a) to form SO_3(a) or SO_4(a) at room temperature [7]. The presence of O_2 in the gas phase was found to accelerate the oxidation of SO_2 on Cu(1 1 1) [8]. The reaction of oxidation of SO_2 has also been shown to be promoted by pre-adsorbed oxygen on Cu(1 0 0) [9]. The oxidation of sulphur dioxide has been well characterised on some oxide surfaces by use of infrared spectroscopy. It has been shown that, depending on the nature and on the structure of the oxide, either bulk-like or surface sulphates can be formed [10]; this is of particular importance for trapping SO_x compounds in some catalytic cracking reactions. Lavalley and his group [11] made clear the mechanism of sulphatation on supported oxides; they identified the vibration modes on sulphates on copper oxide and proposed a mechanism, involving oxygen from the gas phase rather than from the oxide, for their formation. These data already strongly suggest the importance of both the surface structure and the level of oxidation upon the nature of the species formed by adsorption and interaction of sulphur dioxide. Performing experiments on well-defined surfaces and in situ chemical characterisation appears to be a promising way to better understand the mechanism of interaction of SO_2 with metallic and oxide surfaces.

3.2. Experimental results

3.2.1. Surface preparation

Metallic copper surfaces were oriented to within 1° by X-ray back-reflection, mechanically and electrochemically polished. The samples were then annealed under hydrogen at 900 K for 24 h in order to restore the surface and eliminate superficial impurities before being mounted in the UHV chamber. The chemical composition of the surface was checked by AES before every experiment.

The copper surfaces were possibly modified by adsorption of oxygen at 500 K (200×10^{-6} Torr s), or at 800 K (600×10^{-6} Torr s). Long-range ordered structures, consisting of pseudo-unidimensional Cu–O rows along one direction, were formed upon the former treatment. A $(2\sqrt{2} \times \sqrt{2})$R45° and a c(6 × 2) structures were observed by LEED, corresponding to $\theta = 0.5$ and 0.67 ($I_O/I_{Cu60\,eV}$ peak-to-peak ratio equal to 0.2 and 0.25), on the (1 0 0) and the (1 1 0) planes, respectively. The restructuring of these two surfaces is of similar type, they essentially differ by the coverage ($\theta = 0.5$ and 0.67) and the coordinance of the surface oxygen atoms as represented in Schemes 1 and 2. The treatment at 800 K leads to the epitaxial growth of a superficial Cu_2O oxide layer [12] having a (1 1 1) orientation on Cu(1 0 0) and a (1 1 0) one on the Cu(1 1 0) plane. These two oxide structures are characterised by different interatomic distances and surface compositions (see Schemes 3 and 4). The formation of Cu_2O, in the surface layers, has been checked by repeating the same oxidation conditions in the preparation chamber of an apparatus equipped for X-ray photoelectron spectroscopy (XPS) and then by recording corresponding XPS spectra.

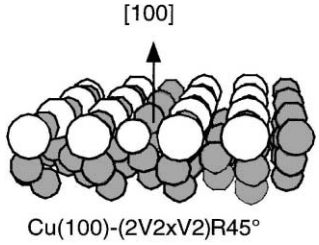

Scheme 1. The notation 'open circles' has been used for O_{ads} atoms and O^{2-} anions, and 'filled circles' for metal atoms or cations, irrespective of the sizes.

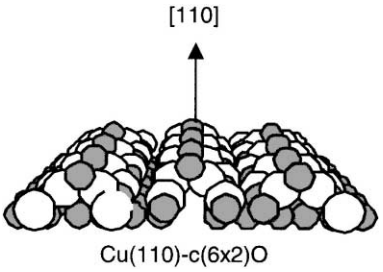

Scheme 2. The notation 'open circles' has been used for O_{ads} atoms and O^{2-} anions, and 'filled circles' for metal atoms or cations, irrespective of the sizes.

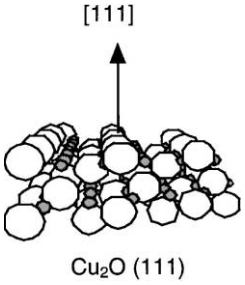

Scheme 3. The notation 'open circles' has been used for O_{ads} atoms and O^{2-} anions, and 'filled circles' for metal atoms or cations, irrespective of the sizes.

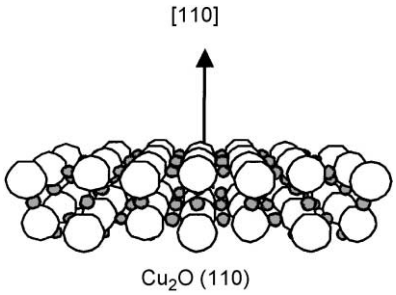

Scheme 4. The notation 'open circles' has been used for O_{ads} atoms and O^{2-} anions, and 'filled circles' for metal atoms or cations, irrespective of the sizes.

Note that copper oxide has a strong ionic character (Cu, +0.86, O, −1.72) and basic properties [13].

In the following, these surfaces will be notified as O_{ads}–Cu(1 0 0) or O_{ads}–Cu(1 1 0) and Cu_2O/Cu(1 0 0) or Cu_2O/Cu(1 1 0).

3.2.2. SO_2 on metallic Cu(1 0 0) and Cu(1 1 0)

The IRAS spectrum of an initially clean Cu(1 0 0) surface was recorded in the presence of sulphur dioxide, $P_{SO_2} = 8 \times 10^{-6}$ Torr at room temperature (see Fig. 2). Vibration bands are observed between 1400 and 900 cm^{-1}, the region of S–O stretching vibrations. The spectrum is dominated by a strong vibration band

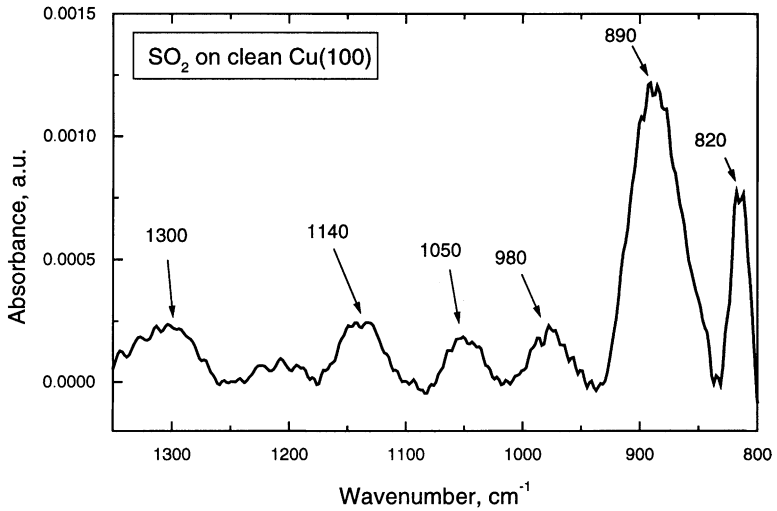

Fig. 2. IRAS spectrum of the metallic Cu(1 0 0) surface after 50 min of SO_2 interaction, $P_{SO_2} = 8 \times 10^{-6}$ Torr.

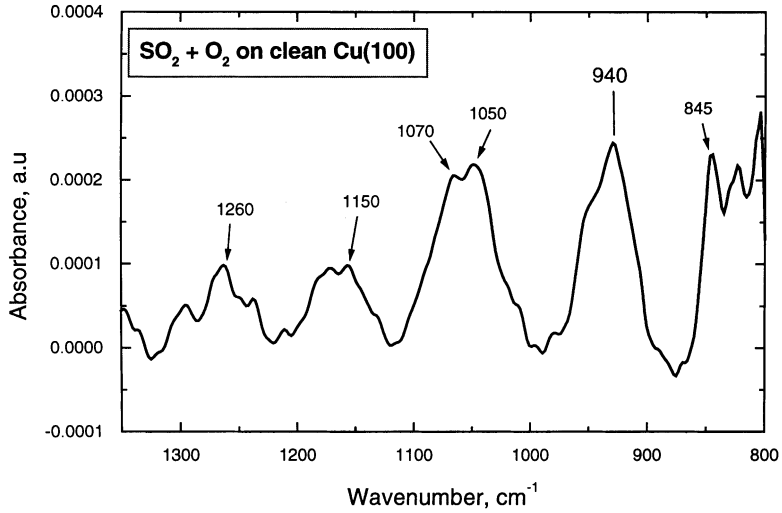

Fig. 3. IRAS spectrum of the metallic Cu(1 0 0) surface after 50 min of $SO_2 + O_2$ interaction, $P_{SO_2} = P_{O_2} = 5 \times 10^{-6}$ Torr.

at 890 cm^{-1}. Five weaker bands are present at 820, 980, 1050, 1140 and 1300 cm^{-1}.

When oxygen was co-adsorbed with sulphur dioxide, $P_{SO_2} = P_{O_2} = 5 \times 10^{-6}$ Torr, new features appear indicating a change in the surface species (see Fig. 3). Vibration bands are now observed at 805, 820, 845, 940–960, 1050–1070, 1150 and 1260 cm^{-1}. The number of vibration bands on spectra of Figs. 2 and 3, six or more, indicates that at least two molecular species have been formed on the surface (an adsorbed sulphate species has, at a maximum, four IR-active stretching bands).

Keeping in mind that bands in reflection spectra may be shifted compared to the same ones in transmission, we tried to be cautious in our interpretations. However, assignment of most of the vibration features could be made based on the literature data related to sulphites and sulphates adsorbed on metal or oxide surfaces and also to bulk complexes where sulphates and sulphites are ligands. It is well established that ionic sulphates have at least one and generally several vibration frequencies above 1100 cm^{-1}, whereas bands at ca. 1050 and 980 cm^{-1}, close to the ones of free sulphite ions indicate the formation of adsorbed sulphites. Moreover, due to metal-adsorbate electron transfer, vibration bands of sulphur-bound sulphites are at higher frequencies than those of free sulphite ions. The opposite trend is true for the oxygen-bound sulphites [14]. Finally, an increase in the number of surface-active bands compared to free ionic entities indicates a lowering of the symmetry and this criterion provides additional information about the nature of the adsorption site and the binding modes of the molecular compounds with the surface.

As a consequence, the two bands at 820 and 890 cm^{-1} are indicative of O-bound sulphites, dominant on the surface, whereas those at 1050 and 980 cm^{-1} are attributed to S-bound sulphites; the presence of the latter implies that SO_2 first interacts with an oxygen surface atom and then binds via its S atom. This change of configuration stabilises the surface entity by increasing its symmetry [15]. The two bands at 1130 and 1300 cm^{-1} are ascribed to S-bound SO and SO_2 species [16], respectively.

The appearance of new bands at ca. 1260 and 940–960 cm^{-1} when oxygen is co-adsorbed with SO_2 indicates the formation of sulphates, bidentate, bound by two adsorbed oxygen atoms, and having two SO bonds characterised by a strong double bond character (see below). Here again is demonstrated the strong reactivity and nucleophilic character of adsorbed oxygen issued from the gas phase [17]. The shift of the sulphite stretching modes, at 845 and 940 cm^{-1}, in the presence of oxygen, is likely to be due to a stronger electron transfer from the oxygen-enriched surface to the S–O bonds. Note that no signal was detected

in the 1350–1400 cm^{-1} region which excludes the existence of disulphites, S_2O_5 [18].

No molecular species were detected upon interaction of SO_2 or $SO_2 + O_2$ ($P = 10^{-5}$ Torr) on Cu(1 1 0). SO_2 essentially dissociates on that surface as confirmed by the increase of both the S and O Auger signal after gas evacuation. This is in agreement with the well-known high reactivity of low coordination surface copper atoms present on this plane [19].

3.2.3. Interaction of SO_2 with oxygen-partially covered Cu(1 0 0) and Cu(1 1 0) surfaces

The IRAS spectra of the oxygen-pre-dosed Cu(1 0 0) and Cu(1 1 0) surfaces were recorded in the presence of sulphur dioxide, $P_{SO_2} = 5 \times 10^{-6}$ Torr. On O_{ads}–Cu(1 0 0) surface ($\theta = 0.5$) (Fig. 4), two groups of broad, and relatively intense, bands grow with exposure at 920–980, 1050, and 1130, 1200, 1275 cm^{-1}, respectively. The first group of bands is very close to the ones of sulphites having three IR-active surface modes; those are likely to be non-symmetric. Note that the broadness of these bands may indicate the interaction of SO_2 with differently bound oxygen atoms, i.e. the oxygen overlayer is not perfectly ordered. The second group of bands, all located at a wavenumber higher than 1100 cm^{-1}, can be ascribed to bidentate sulphates, the asymmetric stretching mode of bulk sulphates having been identified at 1104 cm^{-1} [20] and a binding via two oxygens resulting in a removal of the degeneracy and higher S–O stretching frequencies [21]. On O_{ads}–Cu(1 1 0) surface ($\theta = 0.67$) (Fig. 5), again two groups of bands are observed at similar wavenumbers. However, the vibration bands at high wavenumbers are clearly dominating, indicating that the interaction of SO_2 with such a surface essentially yields sulphate species. The narrowing of the bands, compared to those of Fig. 4, can be explained by an oxygen substructure more ordered on the (1 1 0) than on the (1 0 0) surface [22]. Bands are also more intense due to the higher density and accessibility of oxygen on the c(6 × 2) than on the $(2\sqrt{2} \times \sqrt{2})R45^\circ$ structure.

3.2.4. Interaction of $SO_2 + O_2$ with oxidised Cu(1 0 0) and Cu(1 1 0) surfaces

When a copper oxide, Cu_2O, has been formed on the surface, the interaction of $SO_2 + O_2$ ($P_{SO_2} = P_{O_2} = 5 \times 10^{-5}$ Torr) again leads to the formation of molecular entities, the nature of which appears to be structure dependent. On Cu_2O/Cu(1 0 0) (see Fig. 6), vibration bands are only observed at wavenumbers below 1100 cm^{-1} indicating the exclusive formation of sulphites. On Cu_2O/Cu(1 1 0) (see Fig. 7), the IRAS spectrum is characterised by multiple bands which indicate the co-existence of sulphates and sulphites on the surface. Sulphate bands at 1250, 1150

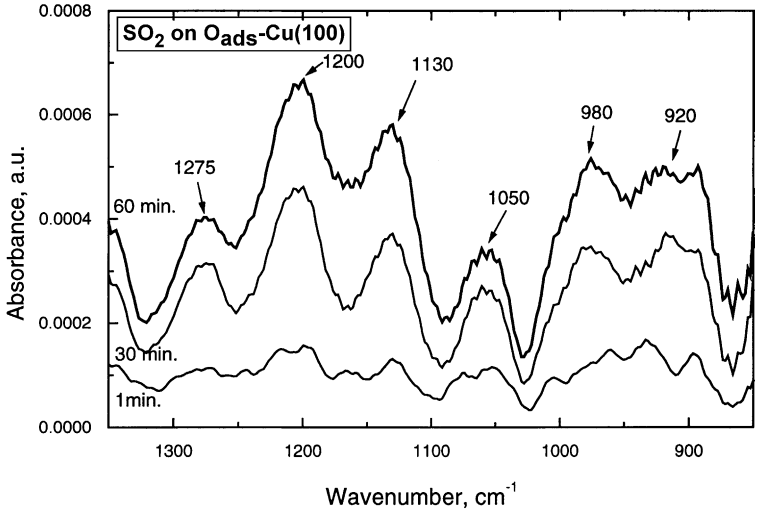

Fig. 4. IRAS spectra of the O_{ads}–Cu(1 0 0) surface, for various times 1, 30 and 60 min, of SO_2 interaction, $P_{SO_2} = 10^{-5}$ Torr.

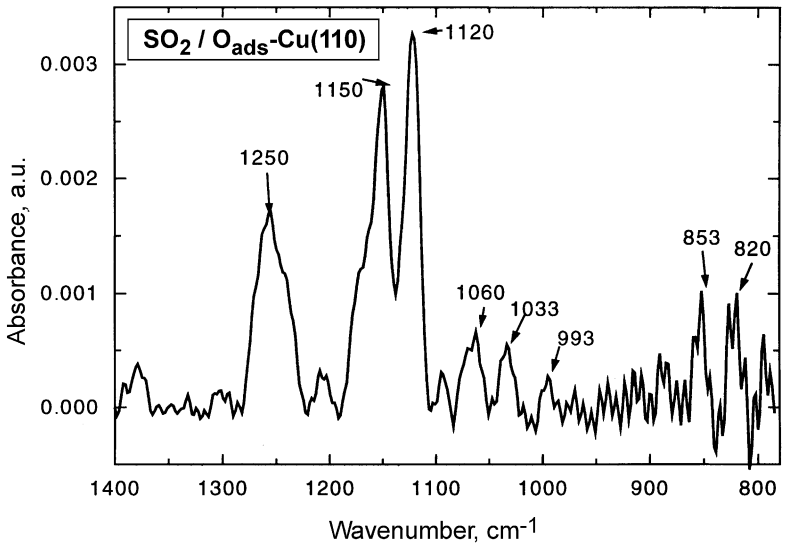

Fig. 5. IRAS spectrum of the O_{ads}–Cu(1 1 0) surface after 50 min of SO_2 interaction, $P_{SO_2} = 10^{-5}$ Torr.

and 1130 cm^{-1} are fingerprints of the formation of bidentate O-bound sulphates [21]. These bands are less intense than on the oxidised Cu(1 0 0) surface.

3.2.5. *Interaction of $SO_2 + C_4H_8$ with the hydroxylated Cu(1 1 0) surface*

This punctual experiment aimed at determining the nature of the surface molecular intermediates under conditions close to the ones used when the NO reduction by isobutene was studied on a copper surface. It was found that addition of 0.2 ppm of sulphur dioxide to a NO + isobutene + oxygen mixture causes a 50% reduction of the rate of NO reduction [23]. Kinetics measurements combined to an XPS characterisation of the catalytic surface led to the conclusion that bulky, oxygen-rich, sulphur species are formed on the Cu(I) surface. In order to find out the nature of the surface species and mimic the reaction conditions, the surface was first hydroxylated by treating the sample under a water pressure of 10^{-5} Torr for

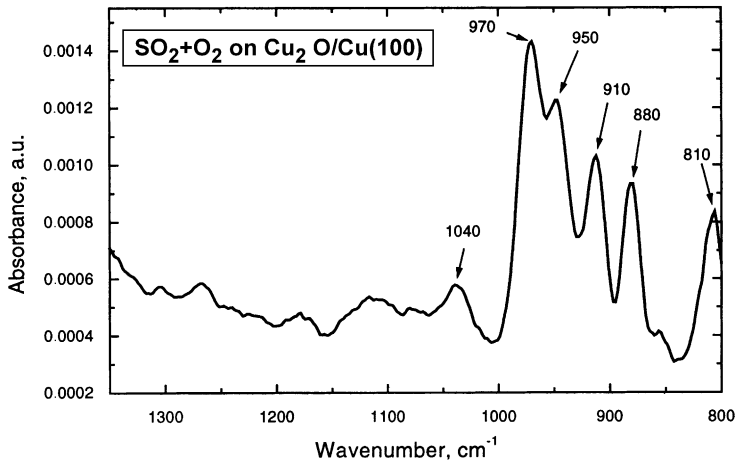

Fig. 6. IRAS spectrum of the oxidised Cu_2O/Cu(1 0 0) surface after 50 min of $SO_2 + O_2$ interaction, $P_{SO_2} = P_{O_2} = 5 \times 10^{-5}$ Torr.

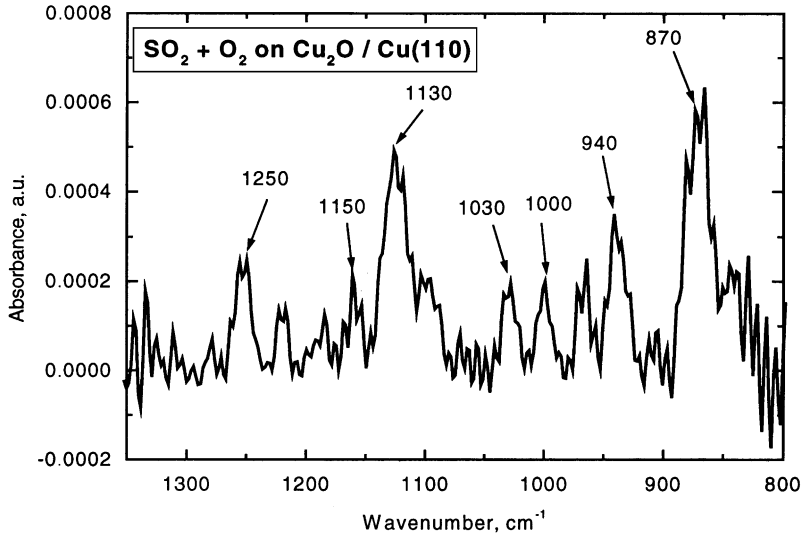

Fig. 7. IRAS spectrum of the oxidised $Cu_2O/Cu(1\,1\,0)$ surface after 50 min of $SO_2 + O_2$ interaction, $P_{SO_2} = P_{O_2} = 5 \times 10^{-5}$ Torr.

a few minutes. Then, sulphur dioxide and isobutene were co-added to the chamber at a total pressure of 10^{-5} Torr (equimolar mixture). The IRAS spectrum (see Fig. 8) reveals that SO_2 does not block the adsorption of isobutene (intense band at around 1665 cm^{-1}). Moreover, the broad IR signal at 1385–1400 cm^{-1} suggests that hydrogen sulphates, HSO_4^-, are formed on the surface [24]. The reaction poisoning is ascribed to the presence of these species that limit the reaction between NO and isobutene rather than to a deep oxidation of the copper as suggested by other authors [25].

3.2.6. Discussion

The main results of the present investigation are summarised in Table 1. The interaction of sulphur dioxide with Cu(1 0 0) and Cu(1 1 0) surfaces leads to very different results showing the role of the structure

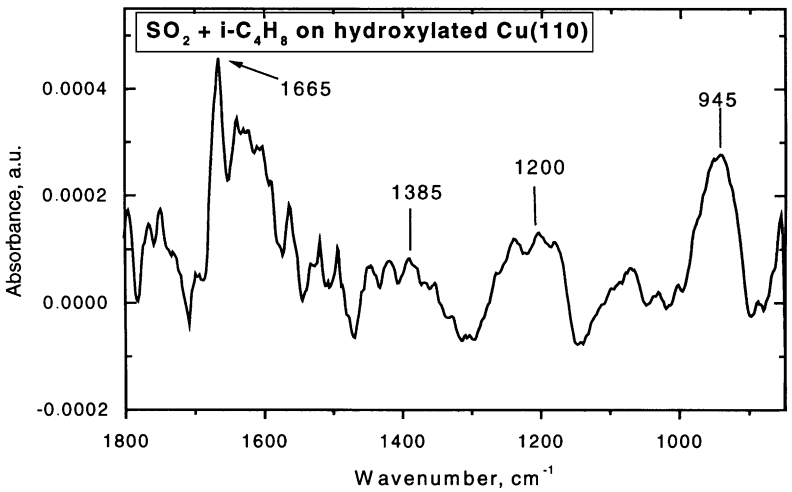

Fig. 8. IRAS spectrum of the hydroxylated Cu(1 1 0) surface after 1 h of $SO_2 + i\text{-}C_4H_8$ interaction, $P_{SO_2} = P_{i\text{-}C_4H_8} = 5 \times 10^{-5}$ Torr.

Table 1
Molecular compounds formed upon interaction of SO_2 or $SO_2 + O_2$ on copper surfaces

Surface	Cu(1 0 0)	Cu(1 1 0)	O_{ads}–Cu(1 0 0)	O_{ads}–Cu(1 1 0)	Cu_2O/Cu(1 0 0)	Cu_2O/Cu(1 1 0)
SO_2 or $SO_2 + O_2$	SO_2, SO_3, SO_4	No molecular adsorption	SO_3, SO_4	SO_3, SO_4	SO_3	SO_3, SO_4

upon the reactivity. The influence of the oxygen reactivity was also evidenced by investigating adsorption of SO_2 on metallic and oxygen-pre-dosed or oxidised surfaces.

Adsorption of SO_2 on the oxygen-pre-dosed Cu(1 1 0) mainly leads to sulphates, whereas sulphites and sulphates are formed on the (1 0 0) one. This can be correlated to the coverage and to the structure of the oxygen overlayers: the coverage is higher on Cu(1 1 0) than on Cu(1 0 0) (0.67 compared to 0.5); the geometric arrangement is favourable to the formation of sulphates on a Cu(1 1 0)-c(6×2)–O structure characterised by O–O first neighbour distance equal to 2.9 Å, compatible with interatomic distances in SO_4^{2-} [22]. Conversely, the $(2\sqrt{2} \times \sqrt{2})R45^\circ$ oxygen substructure, on Cu(1 0 0), provides less accessible oxygen atoms.

The different reactivities, observed on the pre-oxidised surfaces, can also be explained by structural considerations. The Cu_2O(1 1 1) oxide on Cu(1 0 0) is likely to exhibit an oxygen-rich plane under our working conditions with oxygen interatomic distances of 3.7 and 6.09 Å incompatible with two bindings to one impinging SO_2 molecule. This geometry excludes the formation of sulphate species. Conversely, the Cu_2O(1 1 0) oxide, formed on Cu(1 1 0), possesses both metal and oxygen centres accessible to molecules from the gas phase. Oxygen may adsorb in a very reactive form in the vicinity of lattice oxygen; this configuration is thus favourable to the formation of sulphites as a first step and subsequent binding with an additional oxygen atom to form sulphates. This process accounts for the co-existence of sulphites and sulphates on the oxidised Cu(1 1 0) surface.

It is interesting to pay attention to the reactivity of each copper plane as a function of its level of oxidation: on Cu(1 0 0), little differences were observed, both sulphites and sulphates being formed on the metallic or oxygen-precovered surface. When more strongly oxidised into Cu_2O, Cu(1 0 0) gives rise to only sulphites simply because of the geometry of the superficial oxide. On Cu(1 1 0), the influence of oxidation is more striking: the metallic surface induces a complete dissociation of SO_2 whereas pre-adsorbed oxygen makes the same surface able to form sulphates due to the presence of low coordinated, very reactive, surface oxygen atoms. When more oxidised, the same surface becomes less "oxidant" in the sense that both sulphites and sulphates are formed, due to a lower reactivity of surface oxygens embedded in an oxide structure.

Finally, the drastic poisoning effect of SO_2 upon the reaction of NO reduction even when only trace amounts are present in the reactive mixture, can be explained by the formation of bulky molecular species, in strong interaction with, and consequently blocking the reactivity of several surface sites.

All these data are very important for catalytic applications when SO_2 is present; they also show that SO_2 can be efficiently used as a probe molecule for testing the reactivity of a given surface in the presence of oxygen.

3.3. Interaction of NH_3 with copper surfaces

3.3.1. Interaction of NH_3 with metal and oxide surface, a brief literature review

Adsorption of ammonia, often performed to probe the acido-basicity of oxide surfaces, has given rise to a great number of studies [26,27]. However, while extensive experimental and theoretical work has been carried out to characterise the adsorption of NH_3 and the co-adsorption of NH_3 and O_2 either on planar metal and oxide model surfaces at low pressures (10^{-9}–10^{-8} Torr) or on dispersed oxides at much higher pressure, little investigation has been undertaken under intermediate pressure (10^{-6}–10^{-3} Torr). Working under these conditions permits an in situ characterisation of the reaction intermediates on well-defined surfaces and therefore contributes to link high vacuum surface studies and real catalysis.

Beyond the extensively investigated NO reduction process by NH_3, two catalytic reactions, have become real technological challenges: (i) the selective

oxidation of NH_3 into nitrogen and water, now used in modern processes of water depollution; (ii) the deep oxidation of NH_3 into NO for the production of nitric acid. The former reaction is catalysed by transition metal oxides at moderate temperature, and the latter on noble metals at higher temperature. In both processes, the selectivity is a crucial issue since, depending on the experimental conditions, the same catalyst can yield N_2, N_2O or NO as the main product. The knowledge of the mechanism, i.e. of the elementary steps constituting the reaction process, is a key step for the improvement of the catalytic activity and selectivity to the given target products.

Adsorption of ammonia on metal surfaces has been well characterised by using XPS, HREELS, LEED and TDS as well as calculation methods [28]. As examples, ammonia was shown to adopt atop sites with the H atoms pointing away from the surface on Ni(1 1 1), Ni(1 1 0) as well as on Cu(1 1 1) surfaces [29,30]. The binding energy of NH_3 on Cu was shown to arise essentially from electrostatic contributions due to the large dipole moment of NH_3 without significant metal-to-ammonia donation [31]. Experiments, performed on clean copper surfaces at low pressure and temperature, never made clear any dehydrogenation reaction when ammonia was adsorbed alone [32].

Other studies report the role of dioxygen, either in the gas phase or pre-adsorbed, upon the dissociation and the oxy-dehydrogenation of ammonia on metallic surfaces. It has been clearly established that active O_2^- species, transient or precursor surface complexes, participate in the oxy-dehydrogenation of NH_3 much more efficiently than pre-chemisorbed oxygen. This was shown for instance by Afsin et al. [33] on Cu(1 1 0) and Cu(1 1 1). Different reaction pathways were demonstrated to take place depending on the temperature. Selective oxy-dehydrogenation of NH_3 into OH(a) and NH_2(a) species can readily occur at 80 K, NH_3(a) is also present at the surface. At 295 K, imide species are formed by interaction of an ammonia-rich dioxygen–ammonia mixture. At 400 K, the only adsorbed species are NH(a), O_2(a) and N(a). The rate of this process is decreased when the surface oxygen coverage approaches the saturation. The authors come to the extreme conclusion that the growth of a surface oxide layer together with the formation of O^{2-} species makes the surface inactive towards ammonia oxidation. Similar conclusions were drawn by Roberts and co-workers [34] concerning the high reactivity of transient oxygen species towards the oxy-dehydrogenation of ammonia on a Cu(1 1 1) surface. The authors demonstrate that only a very small fraction ($\theta = 0.05$) of preadsorbed oxygen participates in the oxy-dehydrogenation of NH_3 and that the dominant species are imides, NH(a). These imide species were shown to be intermediates to the formation of nitroxyl HNO or to adsorbed nitrogen atoms. They slowly replace O(a) at 295 K when NH_3 interacts with an oxygen-pre-dosed copper surface [35]. The reaction between ammonia and oxygen on Cu(1 1 0) has also been monitored by STM at 300 K. The authors confirmed the role of isolated, preadsorbed oxygen which is progressively replaced by NH(a) species [36]. A theoretical (DFT) approach of the co-adsorption of dioxygen and ammonia on various Cu clusters was presented by Santen and co-workers [37]. The results were the following:

1. Ammonia preferentially adsorbs onefold over a copper cluster model (1 1 1) surface.
2. The presence of oxygen increases the adsorption energy of NH_3 and promotes its dissociation on copper; this is a consequence, first, of the existence of oscillating interactions of copper atoms with oxygen and nitrogen atoms and, second, of a stronger binding of hydrogen atoms with oxygen than with copper.
3. The dissociation of ammonia on a copper surface in the presence of co-adsorbed oxygen mainly results in the formation of NH_2 and OH. These hydroxyls are tilted, about 40°, towards the NH_2 groups (optimal calculated structure).

The easier cleavage of X–H-type bonds by pre-dosed oxygen has also been theoretically demonstrated on copper and other group VIII metals by comparing the reaction enthalpies of the N–H bond breaking when NH_3 is adsorbed on metal (1 1 1) surfaces in the absence and in the presence of pre-adsorbed oxygen [38]. All these conclusions are in remarkable agreement with the majority of experimental data encountered in the literature.

On oxide surfaces, results are numerous and only a short review of the data which may help to discuss our observations will be given here. An interesting correlation has been established between the nature

of the products of ammonia adsorption and the type of acidity of various supported transition metal oxides, chromium, manganese, iron, cobalt, nickel and copper oxides [39]. Ammonia adsorbs in a coordinated form on Lewis-acid sites on all these oxide surfaces; only Cr_2O_3 gives rise to a protonated form on Brønsted acid sites. The authors showed that, on copper oxide, Lewis-coordinated ammonia reacts at room temperature (rt) giving rise to NH imido species, HNO nitrosyl species, N_2^- nitrogen anions and very probably hydrazine depending strongly on the NH_3 partial pressure. N_2H_4 is likely to be an intermediate to the formation of dinitrogen in the selective catalytic oxidation of ammonia (SCO process). Note that all these characterisations have been performed, at rt, after gas evacuation. Additional insights into the surface mechanism were brought by a Russian research team who studied the oxidation of NH_3 at moderate temperature (370–570 K) on Cr_2O_3 and characterised the intermediate species by in situ FT-IR [40]. Two types of reactions were evidenced, one occurring at 370–470 K involving NH_4^+ and one at 470–570 K involving ammonia coordinated to Cr^{3+} cations. In the latter, NO, N_2O and NO_2 are surface intermediates resulting from the interaction of NH_2(a) with O(a). A fundamental study of the interaction of NH_3 with NiO(1 0 0) has been reported by Wu et al. [41]. It is one of the rare studies of the reaction of ammonia oxidation on a well-defined oxide surfaces that could be found in the literature. These authors showed that, on that surface, ammonia is bonded via the N-free electron doublet. The shift of the $\delta_s(NH_3)$ mode (umbrella mode) is ascribed to a net transfer of electrons from ammonia to the metal surface atoms. They also showed that, conversely to what happens on a metallic surface, the shift of the umbrella mode is strictly dependant on the charge of the cations, which are rather isolated on the surface, and not on the NH_3 coverage. This of course validates previous works that made clear a correlation between the acidity of oxide catalysts and the frequency value of the $\delta_s(NH_3)$ vibration mode. Lavalley and his team characterised the adsorption of ammonia on copper oxide supported over alumina. They mainly observed NH_3 coordinated to Lewis-acid sites (bands at 1620 and 1240 cm^{-1} [42] and a minor amount of NH_2^- and NH_4^+ ions (bands at 1450 and 1490 cm^{-1}) resulting from a dismutation of NH_3 on an acid–base pair of sites.

These results show the complexity behaviour of NH_3 in the presence of oxygen on a metallic or an oxidised surface. It is therefore, here again, important to obtain in situ information on well-controlled surfaces to get new insights and clues to understand the reactivity of this system.

3.4. Experimental results

We report here the results obtained on the Cu(1 1 0) surface. Copper has been chosen for its application both in the selective catalytic reduction (SCR process) of NO_x by NH_3 and in the selective catalytic oxidation (SCO process) of ammonia. The (1 1 0) orientation is a model for a dispersed surface characterised by a high fraction of low coordinated atoms.

3.4.1. NH_3 and $NH_3 + O_2$ adsorption on metallic copper

Fig. 9 displays the IRAS spectra recorded on the Cu(1 1 0) crystal surface, for various times, in the presence of ammonia ($P_{NH_3} = 5 \times 10^{-8}$ Torr). One single vibration band was observed in the NH stretching region centred at 3150 cm^{-1}. This feature is associated with the stretching mode of NH, or possibly NH_2, adsorbed species. The experiment was repeated under a higher pressure of NH_3 ($P_{NH_3} = 10^{-3}$ Torr). The obtained spectrum (not shown) was surprisingly modified: only very weak signals were observed indicating very little molecular adsorption. Weak IRAS bands were detected at 1480, 2980 cm^{-1}, characteristic of NH_4^+ ions. We rather believe that this change of reactivity is due to an unavoidable residual amount of water or of oxygen present in the gas mixture despite pumping and heating the gas lines before each experiment. These oxygen or OH surface species, in very low amount, considerably change the surface reactivity. This shows how difficult it is to measure the adsorption of ammonia alone at moderate pressure on a purely metallic surface.

Co-adsorption of NH_3 and O_2, in equal quantities, at total pressure of 5×10^{-6} Torr, leads to a series of spectra, for increasing times of interaction, that are reported in Fig. 10A. All spectra are dominated by an intense band at 2210–2215 cm^{-1}, i.e. remarkably close to that of nitrogen anions, N_2^-, a form of adsorbed molecular dinitrogen [43,44]. Note that the N–N stretching frequency, in complexes containing

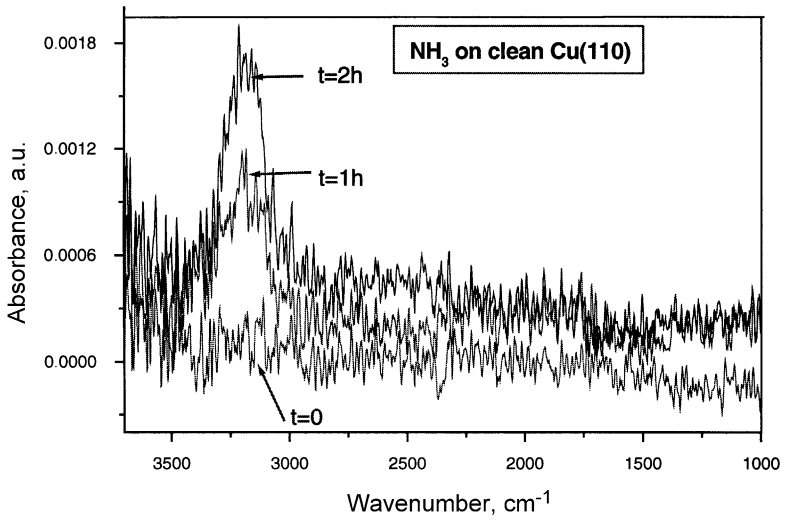

Fig. 9. IRAS spectrum of the metallic Cu(1 1 0) surface during NH_3 interaction, $P_{NH_3} = 5 \times 10^{-8}$ Torr.

metal–N≡N bonds, is known to be comprised between 1930 and 2230 cm^{-1} [45]. The considerable downward frequency shift compared to gaseous dinitrogen (2331 cm^{-1}) has been considered as a proof of chemisorption which induces a π^* back-bonding from the metal surface [46]. Molecular adsorption of dinitrogen has been characterised by IRAS on Pt(1 1 1) and Ni(1 1 0) surfaces; the authors detected an asymmetric IR signal, at low N_2 coverage, which they assigned to multiple components (ordered structure and defect sites). A slight downward shift of the vibration band was observed when increasing the coverage and discussed in terms of dipole and chemical coupling compensation [47,48]. In our experiments, the evolution of the main band, growing with time of exposure, and shifting from a wavenumber close to 2210–2215 cm^{-1} (see Fig. 10B) can be explained by electronic considerations. Isoelectronic to the CO

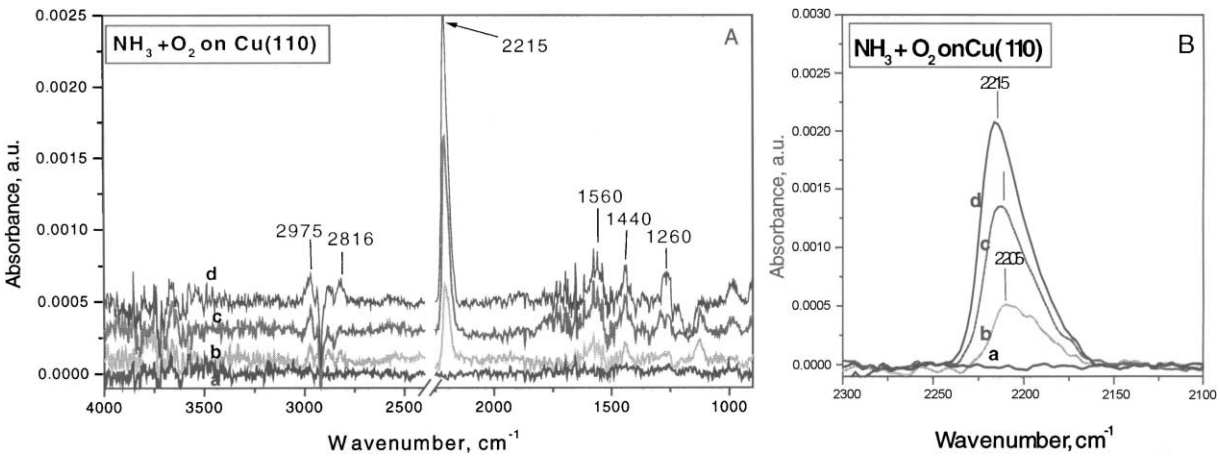

Fig. 10. IRAS spectrum of the metallic Cu(1 1 0) surface during $NH_3 + O_2$ interaction, $P_{NH_3} = P_{O_2} = 10^{-5}$ Torr: (a) 5 min; (b) 1 h 30 min; (c) 2 h; (d) 2 h 30 min. (A) Spectrum between 900 and 4000 cm^{-1}, the *x*-axis has been broken between 2250 and 2400 cm^{-1} in order not to "see" the signal from residual gaseous CO_2. (B) Detailed spectrum around 2200 cm^{-1}.

bond, the N–N one is, as said before, affected by σ_u donation of electrons to the surface acid sites (metal) and to the π back transfer from the metal. Moreover, similar to CO, N_2 has a large dynamic dipole, as indicated by the intense IR signal, that results in a strong dipole–dipole coupling. The small variation in frequency with increasing surface coverage is similar to the behaviour of CO chemisorbed on copper though in opposite sense [49,50]; it is much less intense than the shifts, observed for CO chemisorption on most group VIII metals. The special behaviour of both CO and N_2, on copper, compared to group VIII metals, has been already explained by a nearly total compensation between the increase in frequency due to dipole–dipole coupling (upward shift) and the downward shift due to purely chemical effects. The residual shift is upward for N_2 on copper because, on that metal, belonging to the group I, the purely chemical effect (electron transfer) is smaller than on group VIII metals. Another possible reason for the small frequency shift observed when increasing the coverage is that N_2, weakly adsorbed, diffuses on the surface and form islands, as suggested by the asymmetric shape of the vibration band, so that the local environment of N_2 molecules does not change when increasing the number of islands (no chemical effect); consequently, only a slight dipole–dipole coupling is observed.

Additional weak signals are observed in the –NH deformation region at 1180, 1260, 1440, 1520–1560 cm^{-1} and in the –NH stretching region at 2816, 2880 and 2975 cm^{-1}. These indicate the adsorption of NH_3 coordinatively on metal atoms (δ_{asym} and δ_{sym} at 1580 and 1180 cm^{-1}, respectively) and its reactivity with oxygen to yield amide species, NH_2(a) (shoulder at 1520 cm^{-1}). The band at 1440 is not straightforward to ascribe: it could reveal the formation of ammonium ions, NH_4^+, as a result of a dismutation of NH_3 on a Lewis-acid–base pair site; the formation of a small amount of ammonium ions seems to be confirmed by the appearance of weak bands at 2816–2975 cm^{-1} (ν_{NH} in NH_4^+). Growing together with the band at 1260 cm^{-1}, we are inclined to think that the vibration mode at 1440 cm^{-1} mainly originates from the transformation of adsorbed NH_3 into hydrazine, N_2H_4. Such a reaction has been already evidenced after adsorption and oxidation of ammonia on CuO–TiO_2 and assignments were confirmed by adsorption of pure hydrazine [43]. This is in perfect agreement with the redox-type mechanism proposed by Ramis et al. [51] for the formation of dinitrogen on CuO/TiO_2; it implies the oxy-dehydrogenation of NH_3 into NH_2(a), the formation of hydrazine and finally its decomposition into N_2, H^+ and electrons that may reduce the cationic centres formed upon oxygen interaction. The intensity of these bands never exceeds 5×10^{-4} a.u. suggesting that, under our conditions, there is, anyway, little adsorption of NH_4^+, N_2H_4 or NH_x compounds on a metallic copper surface. $N_2^{\delta-}$ (or N_2) is far the dominant adsorbed product. Moreover, conversely to the net increase with time of the band at 2200 cm^{-1}, the other IR signals are almost unchanged throughout the exposure. They are possibly associated with reaction intermediates for the formation of N_2; their concentration is thus stationary on the surface. Evacuation of the reacting mixture only slightly reduces the signal at 2115 cm^{-1}. The sample was finally heated in vacuum (10^{-8} Torr) to 473 K for 5 min and cooled back to room temperature. The vibration at 2215 cm^{-1} totally disappears upon this treatment. Finally, under these conditions, we did not detect any band in the 1800–2000 cm^{-1} region. This rules out the formation of NO or any NO-containing species. No evidence was either obtained for OH formation on the surface.

This new sets of data proves the enhanced reactivity of the copper surface towards NH_3 adsorption, abstraction of hydrogen and finally recombination of adsorbed N atoms or NH species, when it is submitted to oxygen together with NH_3. At 295 K, the dissociation of oxygen provides "hot", very reactive, oxygen atoms, which participate in the reaction of oxy-dehydrogenation of NH_3 by abstraction of protons [34].

3.4.2. $NH_3 + O_2$ on oxygen-pre-dosed Cu(1 1 0)

This experiment aimed at characterising the reactivity of weakly bound oxygen atoms. The clean Cu(1 1 0) surface was first submitted to 200 l of oxygen at 500 K in order to adsorb a fraction of monolayer of oxygen ($\theta = 0.67$) [22]. An equimolecular mixture of ammonia and oxygen (total pressure $= 2 \times 10^{-5}$ Torr) was then admitted onto the sample and the IRAS analysis was performed in situ. The spectra are shown in Fig. 11. Similarly to what has been observed on the initially metallic surface, an IR signal appears at ca. 2210 cm^{-1}, grows and shifts upwards with increasing

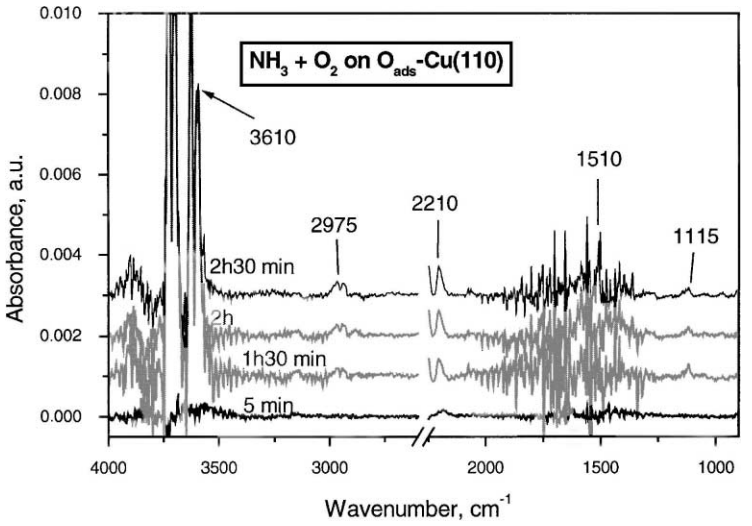

Fig. 11. IRAS spectrum of the O_{ads}–Cu(1 1 0) surface during $NH_3 + O_2$ interaction, $P_{NH_3} = P_{O_2} = 10^{-5}$ Torr. The *x*-axis has been broken between 2250 and 2400 cm^{-1} in order not to "see" the signal from residual gaseous CO_2.

exposure. It is attributed to $N_2{}^{\delta-}$ species. For similar exposure, it is half as small as in the previous case indicating a corresponding decrease in the amount of dinitrogen adsorbates. Intense and broad bands appear at 3600 and 3800 cm^{-1} showing the formation of a large amount of hydroxyls. OH groups were not detected in Fig. 10 either because they recombined into water and desorbed or because they were tilted towards NH_2 groups and hence IR-inactive. In this case, adsorbed hydroxyls seem to be stabilised by pre-adsorbed oxygen; these groups are likely to limit the recombination of NH_x species into N_2H_4 then N_2. The two bands, at 3600 and 3800 cm^{-1}, may also be assigned to isolated O-adsorbed H_2O molecules which would similarly limit the surface reaction.

3.4.3. Adsorption of dinitrogen on Cu(1 1 0)

Adsorption of dinitrogen was investigated on the oxygen-pre-dosed surface ($\theta = 0.67$). The obtained spectra, for various times of exposure under a nitrogen pressure of 5×10^{-5} Torr, are given in Fig. 12. A broad vibration feature appears and grows at ca. 2210 cm^{-1} upon exposure at room temperature. A shoulder at ca. 2184 cm^{-1} starts growing after 80 min. The appearance of a main signal at ca. 2210 cm^{-1} confirms its assignment to $N_2{}^{\delta-}$ species above proposed for the adsorption of NH_3 in the presence of oxygen. We may ascribe the second signal to adsorption at another type

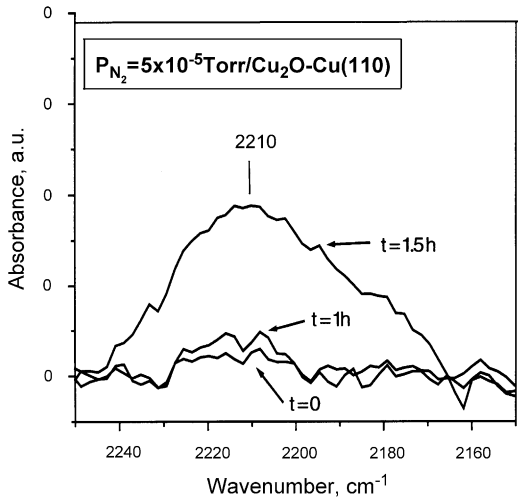

Fig. 12. The 2245–2150 cm^{-1} region of the IRAS spectrum of the oxidised Cu_2O/Cu(1 1 0) surface during dinitrogen interaction, $P_{N_2} = 5 \times 10^{-5}$ Torr.

of site or to the interaction of some tilted $N_2{}^{\delta-}$ with another metal centre.

4. Conclusions

The adsorption and oxidation of two complex molecules, SO_2 and NH_3, could be monitored in situ

by FT-IRAS on model copper surfaces. Great similarities have been observed in the reactivities of these two molecules. These are highly sensitive to the surface structure and to the oxidation level of the surface. These two probe molecules reveal the special reactivity of weakly bound oxygen compared to the same species embedded in an oxide structure.

On Cu(1 1 0), low coordination atoms favour the dissociation of SO_2 into adsorbed oxygen and sulphur. Sulphites and sulphates, coordinated to the surface via oxygen have been identified during interaction of SO_2 with Cu(1 0 0), oxygen-precovered Cu(1 1 0) surfaces or oxidised Cu(1 0 0) and Cu(1 1 0) surfaces.

The adsorption and interaction with oxygen of ammonia on Cu(1 1 0) also yield various molecular compounds, coordinated NH_3, NH_2, N_2 as well as NH_4^+ and OH^-, depending on the oxygen addition procedure. It appears that the presence of oxygen in the gas phase activates the N–H bond cleavage which is followed either by N–N recombination or by interaction of NH_3 with surface OH to form surface NH_4^+ species.

This set of data presented here prove the great potential of IRAS for in situ surface reactivity studies.

Acknowledgements

I acknowledge my colleagues, A. Adamski, P. Dubot, E. Jacqueson and C. Méthivier, for their contribution to the recent results presented above.

References

[1] R.G. Greenler, J. Chem. Phys. 44 (1966) 310.
[2] A.M. Bradshaw, F.M. Hoffmann, Surf. Sci. 72 (1978) 513.
[3] F.M. Hoffmann, Surf. Sci. Rep. 3 (1983) 107.
[4] M.A. Chesters, S.F. Parker, R. Raval, Surf. Sci. 165 (1986) 179.
[5] J. Szanyi, W.K. Kuhn, D.W. Goodman, J. Vac. Sci. Technol. A 11 (1993) 1969.
[6] K. Horn, J. Pritchard, J. Phys. 38 (1977) C4–C164.
[7] M. Polcik, L. Wilde, J. Haase, B. Brena, D. Cocco, G. Comelli, G. Paolucci, Phys. Rev. B 53 (1996) 13720.
[8] J.P. Baxter, M. Runze, C.W. Kong, J. Vac. Sci. Technol. A 6 (1988) 1123.
[9] H. Lu, E. Janin, M.E. Davila, C.M. Pradier, M. Gothelid, Vacuum 49 (1998) 171.
[10] M. Bensitel, M. Waqif, O. Saur, J.C. Lavalley, J. Phys. Chem. 93 (1989) 6581.
[11] M. Waqif, O. Saur, J.C. Lavalley, S. Perathoner, G. Centi, J. Phys. Chem. 95 (1991) 4051.
[12] A.P. Baddorf, J.F. Wendelken, Surf. Sci. 256 (1991) 264.
[13] T. Bredow, G. Pacchioni, Surf. Sci. 373 (1997) 21.
[14] F.A. Cotton, F.J. Francis, J. Am. Chem. Soc. 82 (1960) 2986.
[15] C.C. Chang, J. Catal. 53 (1978) 374.
[16] G.J. Kubas, Inorg. Chem. 18 (1979) 182.
[17] B. Afsui, P.R. Davies, A. Pashusky, M.W. Roberts, D. Vincent, Surf. Sci. 284 (1983) 109.
[18] J.C. Lavalley, Catal. Today 27 (1996) 377.
[19] D. Spanjaar, M.C. Desjonquères, Concepts in Surface Physics, Surface Science Series, Springer, New York, 1994.
[20] K. Nakamoto, J. Fujita, S. Tanaka, M. Kobayashi, J. Am. Chem. Soc. 79 (1957) 4904.
[21] D.A. Outka, R.J. Madix, G.B. Fisher, C. DiMaggio, J. Phys. Chem. 90 (1986) 4051.
[22] F. Besenbacher, J.K. Norskov, Oxygen Chemisorption on Metal Surfaces: General Trends for Cu, Ni and Ag, Pergamon Press, Oxford, 1993.
[23] H. Lu, C.M. Pradier, A.S. Flodstrom, J. Mol. Catal. A 112 (1996) 459.
[24] A. Patel, G. Coudurier, N. Essayem, J.C. Vedrine, J. Chem. Soc., Faraday Trans. 93 (1997) 347.
[25] M. Iwamoto, H. Yahiro, K. Tanda, Stud. Surf. Sci. Catal. 37 (1988) 219.
[26] J.C. Lavalley, Catal. Today 27 (1996) 377.
[27] H. Knozinger, Elementary Reaction Steps, Kluwer Academic Publishers, Dordrecht, 1993.
[28] A. Chattopadhyay, H. Yang, J.L. Whitten, J. Phys. Chem. 94 (1990) 6379.
[29] L.E. Dastoor, P. Gardner, D.A. King, Surf. Sci. 289 (1993) 279.
[30] P. Baumgartel, R. Lindsay, T. Giessel, O. Schaff, A.M. Bradshaw, D.P. Woodruff, J. Phys. Chem. 104 (14) (2000) 3044.
[31] P.S. Bagus, K. Hermann, Phys. Rev. B 33 (1986) 2987.
[32] D. Lackey, M. Surman, D.A. King, Vacuum 33 (1983) 867.
[33] B. Afsin, P.R. Davies, A. Pashusky, M.W. Roberts, D. Vincent, Surf. Sci. 284 (1993) 109.
[34] A. Boronin, A. Pashusky, M.W. Roberts, Catal. Lett. 16 (1992) 345.
[35] D.M. Thornburg, R.J. Madix, Surf. Sci. 220 (1989) 268.
[36] X.-C. Guo, J.M. Madix, Surf. Sci. 387 (1997) 1.
[37] G.J.C.S.V.d. Kerhof, W. Biemolt, A.P.J. Jansen, R.A.v. Santen, Surf. Sci. 284 (1993) 361.
[38] E. Shustorovich, A.T. Bell, Surf. Sci. 268 (1992) 397.
[39] J.M. Gallardo Amores, V.S. Escribano, G. Ramis, G. Busca, Appl. Catal. B 13 (1997) 45.
[40] V.A. Matyshak, O.N. Sil'chenkova, I.N. Staroverova, V.N. Korchak, Kinet. Catal. 5 (1995) 677.
[41] M.-C. Wu, C.M. Truong, D.W. Goodman, J. Phys. Chem. 97 (1993) 4182.
[42] A.A. Tsyganenko, D.V. Pozdnyakov, V.N. Filimonov, J. Mol. Struct. 29 (1975) 299.
[43] G. Ramis, L. Yi, G. Busca, M. Turco, E. Kotur, R.J. Willey, J. Catal. 157 (1995) 523.
[44] J.M.G. Amores, V.S. Escribano, G. Ramis, G. Busca, Appl. Catal. B 13 (1997) 45.

[45] F.A. Cotton, G. Wilkinson, Advanced Inorganic Chemistry, 3rd Edition, Wiley, New York, 1972.
[46] D.A. King, Surf. Sci. 9 (1968) 375.
[47] M.E. Brubaker, M. Trenary, J. Chem. Phys. 85 (1986) 6100.
[48] R.A. Shigeishi, D.A. King, Surf. Sci. 62 (1977) 379.
[49] P. Hollins, J. Pritchard, Surf. Sci. 89 (1979) 486.
[50] B.E. Hayden, K. Kretzschmar, A.M. Bradshaw, Surf. Sci. 155 (1985) 553.
[51] G. Ramis, L. Yi, G. Busca, Catal. Today 28 (1996) 373.